

ADVANCES IN THE CIRCUMSTELLAR MEDIUM

G. García-Segura¹

RESUMEN

Se discuten avances recientes en cómputo hidrodinámico del medio circunestelar, los cuales son útiles para comprender, por ejemplo, algunas características observadas en estallidos largos de rayos gamma.

ABSTRACT

We discuss recent advances in hydrodynamical computations of the circumstellar medium, which are useful to understand, for example, some features observed in long gamma ray bursts.

Key Words: circumstellar matter — hydrodynamics — ISM: bubbles — planetary nebulae: general — planetary nebulae: individual (NGC 1360) — stars: evolution

1. PLANETARY AND PROTO-PLANETARY NEBULAE: SHAPES AND DYNAMICS

The inclusion of a weak magnetic field in a line-driven wind results in a very powerful tool to understand many of the dynamical processes involved in WR bubbles and planetary nebulae (PNs), such as the case of the extreme collimation that present many PNs and proto-PNs. Chevalier & Luo (1994) made thin-shell, semi analytical solutions to explore the effects of a rotating star with a magnetized wind on the formation of aspherical bubbles. Following this scheme, Różyczka & Franco (1996) and García-Segura et al. (1999a), performed 2-D MHD simulations of magnetized winds in cylindrical and spherical geometries, respectively, showing that the magnetic tension may indeed be responsible for the generation of jets in PNs. García-Segura (1997) presented full 3-D MHD models of PNs where jets and ansae are convincingly reproduced as the result of magnetic collimation of the post-AGB wind. The success of the inclusion of magnetic fields is also shown in García-Segura et al. (2005) for the case of proto-PNs.

An example is shown in Figure 1, which shows that MHD simulations can be extremely successful in reproducing all kind of complicated features in PNs, such as the case of NGC 6543, a bipolar nebula, with an internal elliptical bubble, precessing jets, and ansae.

2. NGC 1360: A TEST CASE OF MAGNETIC COLLIMATION

NGC 1360 is an interesting planetary nebula for several reasons. Firstly, this is one of the few plane-

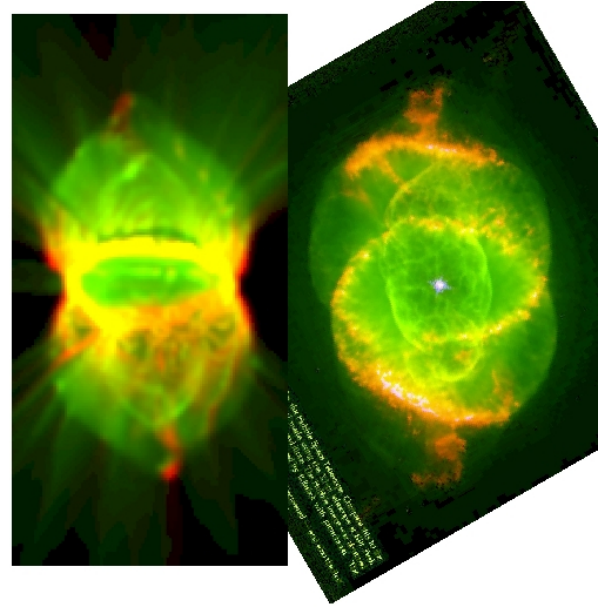


Fig. 1. An example of a 3-D MHD simulation compared with the HST image of NGC 6543.

tary nebulae where an intense stellar magnetic field, of the order of kilogauss, has been detected in its core (Jordan et al. 2005). Secondly, the nebula shows an elongated and nearly featureless morphology with no apparent bright rim, sharp inner boundary or central cavity, indicating the current absence of a significant stellar wind, this is further confirmed by archive IUE spectra of the core of NGC 1360 that reveal the absence of P Cygni-type line profiles. Furthermore, the nebula has a system of fast-expanding bipolar jets outside the main nebular body.

Although NGC 1360 had been classified by Méndez & Niemela (1977) as containing a close bi-

¹Instituto de Astronomía, Universidad Nacional Autónoma de México, Apdo. Postal 877, 22800 Ensenada, B. C., Mexico (ggs@astro.unam.mx).

nary nucleus, Wehmeyer & Kohoutek (1979) were unable to confirm such claim after a detailed radial velocity study of the central star. More recently, Goldman et al. (2004) have described NGC 1360 as a thick shell without a sharp inner edge that indicates a lack of ongoing compression by a fast stellar wind. They also have brought attention to the presence of the bipolar jets and studied the kinematics of the shell and the northern jet. The central region of NGC 1360 shows no $[\text{N II}] \lambda 6548, 6584$ emission lines, these lines are only detected on the strings of knots that form the system of bipolar collimated outflows, which from an isolated knot located on the northern edge of the nebula in our data. Since collimated, bipolar outflows in planetary nebulae are thought to originate either from the action of binary nuclei or magnetic fields, and given the lack of evidence of the former and the high significance of the observations of the latter in this case, NGC 1360 represents a unique case to test the possible effects of a magnetic collimation process in the development of this object. Furthermore, recently García-Segura et al. (2006) have started exploring the expected structure of planetary nebulae once the fast wind has faded, and NGC 1360 represents also an opportunity to examine the characteristics of this stage.

Relevant data for NGC 1360 are its high electron temperature $T_e [\text{O III}] = 16500 \text{ K}$ and low electron density $N_e \lesssim 100 \text{ cm}^{-3}$ (Kaler, Shaw, & Kwitter 1990); high effective temperature $T_{\text{eff}} = 97\,000 \text{ K}$, $\log L = 3.64 L_{\odot}$, $M = 0.65 M_{\odot}$, main sequence mass $M_{\text{ms}} = 2.7 M_{\odot}$ (Traulsen et al. 2005; Jordan et al. 2005). A distance estimate determined from *Hipparcos* data (Acker et al. 1998) $d = 350 \pm \frac{1000}{180} \text{ pc}$ is adopted here.

NGC 1360 presents us with a rather peculiar situation: it shows no signs of having a binary system, it has a bipolar jet system, the fast stellar wind has faded and the central star of NGC 1360 has a substantial magnetic field. Under these circumstances we have explored the case of magnetic collimation during the development of this planetary nebula to try to understand its structural and kinematic evolution, including the history of the bipolar collimated outflows. We note, however, that the current lack of evidence for the presence of a binary nucleus does not preclude it from having existed at earlier stages, e.g. during the AGB phase and having merged after a common envelope interaction. In any case, the current rotational velocity of the central star is quite moderate, as expected for a single white dwarf and does not provide clues to the possible early binary interaction.

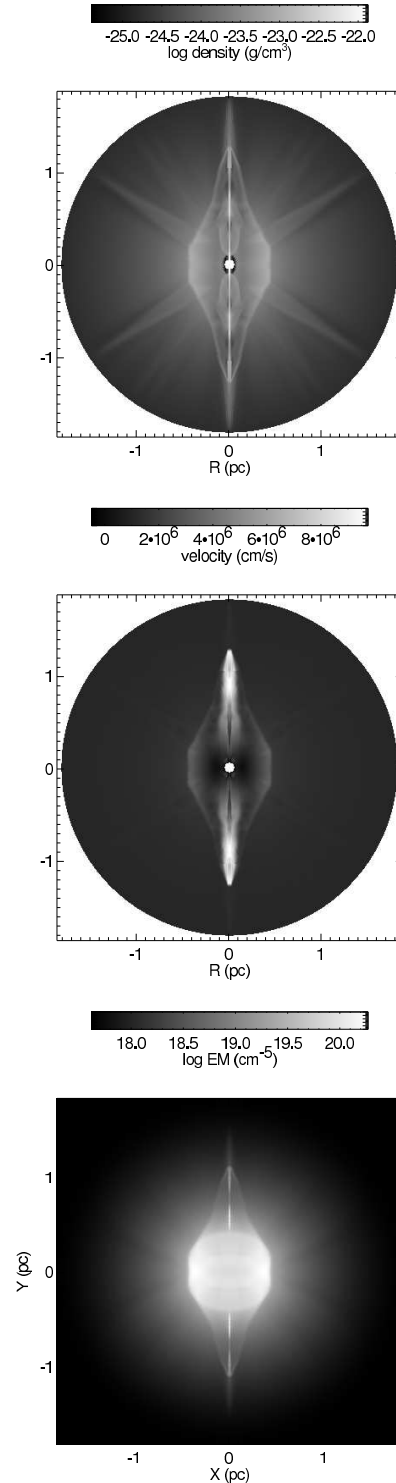


Fig. 2. Snapshot of the NGC 1360 model at 11,000 yrs. Top panel: gas density; middle panel: radial velocity; bottom panel: emission measure of the gas, as projected with a 30° tilt from the plane of the sky.

The MHD simulations presented by García-Díaz et al. (2008) were performed with the hydrodynamical code ZEUS-3D (version 3.4) (Stone & Norman 1992; Clarke 1996) and details about the set up can be found there and in García-Segura et al. (1999a) and García-Segura, López, & Franco(2005) for the self-expanding grid technique.

The current characteristics of NGC 1360 are best reproduced when the model reaches 11,000 yrs, as shown in Figure 2 for the gas density, radial velocity and emission measure of the gas when considering a 30° (Goldman et al. 2004) tilt from the plane of the sky for the nebula.

Goldman et al. (2004) derived a simple kinematic age of ≈ 5000 years for the jets of NGC 1360 which implies that the jets were launched with constant velocity when the nebula was already well developed at half its current kinematic age and at a time when the fast stellar wind was probably starting to weaken. This would indeed be a rare case since jet formation is expected to occur during the very early stages of development of the planetary nebula, right at the end of the AGB stage. To trace the evolution of the model in velocity, 1-dimensional plots of radial velocity *vs* distance from the central star along the polar axis are shown in Figure 3 for time intervals of 10^3 yrs. The velocities and distances for the individual knots in the northern jet have been plotted in this figure as solid squares, (notice that the velocities plotted are $V_{\text{hel}} - V_{\text{sys}}$, i.e. heliocentric minus systematic) showing a very good fit for the model at $\sim 11,500$ yrs. Again, these velocity plots take into account a 30° tilt with respect to the plane of the sky. The plot provide a good explanation of the current state of the jets, their origin as launched by the magnetized stellar wind, their current location, observed increasing outward velocities, and conciliate their age with that of the nebula.

3. MASSIVE STARS: LONG-GAMMA-RAY BURST IN CONSTANT DENSITY MEDIUM

The evolution of a star, imprinted in its location on the Hertzsprung-Russell diagram (HRD) is a basic key to understand the formation and evolution of structures in the circumstellar medium (CSM), such as bubbles and swept-up shells. When stars have high temperatures they are relatively compact (small radius $\sim R_\odot$), and their wind velocities (\propto escape velocities) are of the order of $\sim 10^3 \text{ km s}^{-1}$. On the other hand, when stars have low temperatures, their radii are large ($\sim 10^2 - 10^3 R_\odot$), and their wind velocities (escape velocities) are relatively small, of the order of $\sim 10^1 - 10^2 \text{ km s}^{-1}$. Then, every time

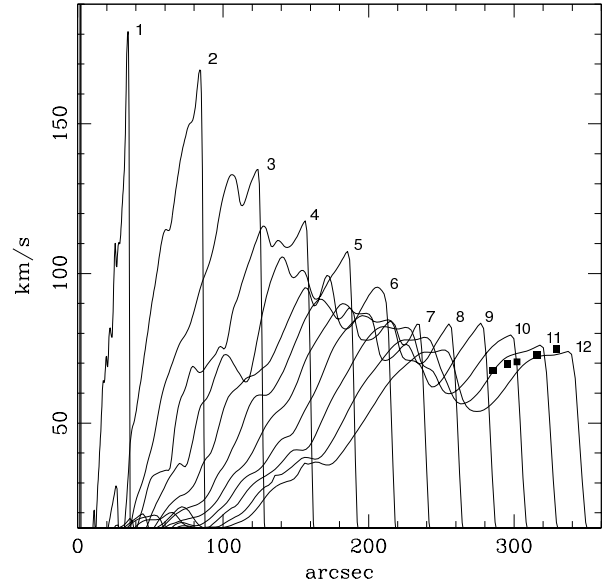


Fig. 3. Velocity *vs* distance from the central star plots for the NGC 1360 model along the polar axis for time intervals in units of 10^3 yrs. The individual northern knots are shown as solid squares.

that a slow wind evolves into a fast wind, a swept-up shell is formed.

The theory of wind blown bubbles is well represented by the Weaver's et al. (1977) paper (30 years of success), and it was thought for main sequence (MS) stars with fast winds sweeping up the ISM. Their analytical solutions gives a good insight for the dynamics of the interaction MS stars \rightarrow ISM, assuming that the MS wind is constant (which is a good approximation). However, most nebulae surrounding stars do not belong to this scenario (only a few of them, such as the case of the bubble nebula NGC 7635), and post-MS evolution has to be taken into account, with time dependent winds.

An effort to couple stellar evolution calculations with the CSM evolution by using hydrodynamical simulations have been made for several stellar models: $12 M_\odot$ (Chita et al. 2007), $20 M_\odot$ (van Marle et al. 2008), 23, 28, 29, 30 and $33 M_\odot$ (Pérez-Rendón et al. 2009), 35 and $60 M_\odot$ (García-Segura et al. 1996a,b), and for low and intermediate stellar masses, 1, 1.5, 2, 2.5, 3.5 a $5 M_\odot$ (Villaver et al. 2002ab). All these studies follow the same scheme which is shown in Figure 4. Although it is still premature, the goal of this scheme is to provide a feedback for the stellar evolution calculations, as denoted by the question mark in Figure 4.

The bubbles surrounding Wolf-Rayet (WR) stars are the best laboratories to study the predictions

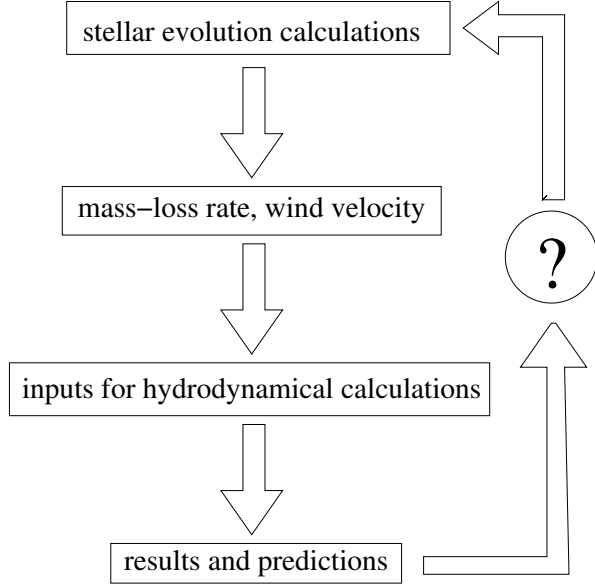


Fig. 4. Logical scheme in CSM computations.

made by the wind blown bubble theory. The analytical solutions by García-Segura & Mac Low (1995), which are an extension of Weaver's et al. (1977) solutions for power laws, give a good insight for the dynamics of the interaction $WR \rightarrow$ red-supergiants. X-ray observations proved the existence of 10^6 K plasma inside the bubbles (such as NGC 6888, Bochkarev 1988; and S308, Chu et al. 2003), as well as UV observations confirmed the existence of conduction fronts (Borosso et al. 1997).

Recently, new discoveries in long gamma ray bursts, in particular, the detection of interstellar absorption lines on top of the emission from the afterglow, have turn the attention again into these WR bubbles. The observed groups of lines, with blue shifted velocities up to ~ 3000 km s $^{-1}$ respect to the afterglow, are thought to originate in the WR wind progenitor and in previous interactions of the CSM (see van Marle et al. 2005 for further details and references therein). Thus, these observations show, in detail, the whole previous evolution of the CSM around long gamma ray burst progenitors.

There is still a dynamical problem with wind blown bubbles, in particular with WR bubbles. If we use the mechanical luminosity (either theoretical or from observations) as input to explain the dynamics, the swept-up shells would expand faster by a factor of 2, the expected x-ray luminosities and the O VI column densities would be larger by a factor of 10. However, if we consider as inputs the expansion velocity of the swept-up shell and the swept-up

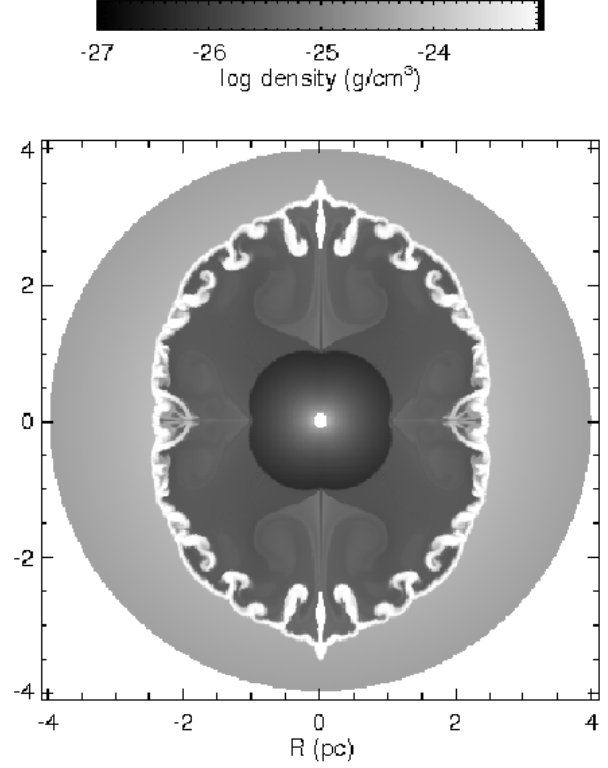


Fig. 5. Magnetized WR bubble with $\sigma = 0.00035$.

mass, the expected X-rays and OIV column densities are well predicted, but the needed mechanical luminosity is a factor of 10 smaller. Thus, there is still a controversy about the measurements of the mass loss rates for WR stars (see for example García-Segura & Mac Low 1995, for the case of the WR bubble NGC 6888).

Since MHD computations are successful, for example in PNs, we can make predictions for other kind of objects, such as WR bubbles and long gamma ray burst (LGRBs) progenitors. The key parameter is σ , the ratio of the magnetic energy to the kinetic energy in the wind, defined as:

$$\sigma = \frac{B^2}{4\pi\rho v_\infty^2} = \frac{B_s^2 R_s^2}{M v_\infty} \left(\frac{v_{\text{rot}}}{v_\infty} \right)^2. \quad (1)$$

Note that σ is very sensitive to the rotation velocity, and this is the point in the present discussion. It is easy to produce models that fit with galactic WR bubbles like NGC 6888, with very small values for σ , as it is shown in Figure 5 (García-Segura et al. 1999b). However, with just a slight increase in the value of the rotational velocity, σ can be incremented to values of 0.01, like the model shown in Figure 6. By doing this, we obtained an elongated bubble, that

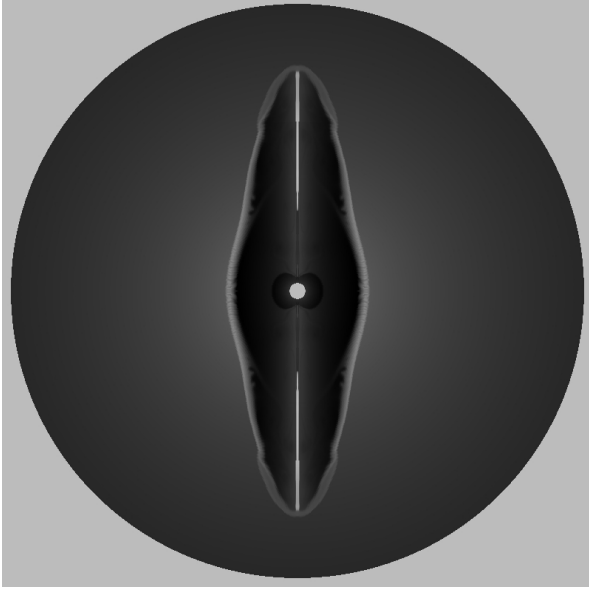


Fig. 6. Magnetized WR bubble with $\sigma = 0.01$.

probably does not match galactic observations, but it has an important feature in the context of LGRBs. This is the position of the reverse shock at the polar regions, which is the region that is going to decelerate the relativistic jet coming from the LGRB. Note that the reverse shock in the magnetized model is much closer to the star (compare Figure 6 with 5), almost a factor of 10. Figure 6 does not have labels, but the spatial dimension is similar to Figure 5. Note that after crossing the reverse shock in the polar direction, the density is rather constant, with larger values than the rest of the bubble due to the hoop stress that pills it up. Note also that, for large enough values of σ , winds are self-collimated at the rotation axis before the reverse shock, producing constant density media even closer to the stellar surface (García-Segura et al., in prep.). There is a controversy about why some LGRB jets appears to slow down in a constant medium (van Marle et al. 2006, and references therein), and others in a free expanding wind like r^{-2} . This is illustrated in Figure 7. The LGRBs that show a constant medium around appear to be at higher redshift, while those that decelerate in a free wind appear to be closer to us. Since there is a correlation between redshift and metallicity, stars at higher redshift would have lower metallicities. But this also means that, the mass-loss rate from these stars would be smaller, and so the angular momentum lost in the winds. Thus, this scenario favors the idea that these stars do not slow down their rotational velocities during the evolution so effective

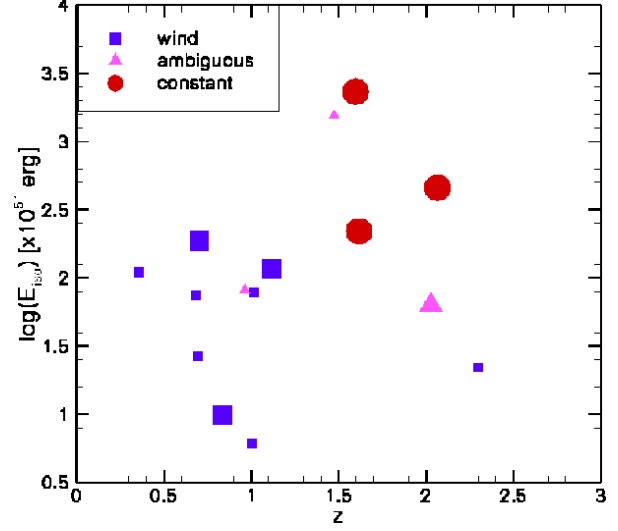


Fig. 7. Type of CSM revealed by afterglows from LGRBs over the redshift-isotropic energy space (van Marle et al. 2006).

as the stars with higher metallicities. From here, it is expected that, at lower metallicities (higher redshift), the MHD effects, and the importance of σ could be notorious, giving a natural explanation for Figure 7. The larger luminosity is also correlated with the larger densities closer to the central stars.

4. CONCENTRIC RINGS AROUND AGBS AND PNS

The multiple concentric rings, or arcs, that were recently discovered by the Hubble Space Telescope around a handful of planetary nebulae is one of the most puzzling and unexpected results delivered by the HST (see Kwok, Su, & Hrivnak 1998; Hrivnak, Kwok, & Su 2001; Terzian & Hajian 2000, and references therein). The best documented case of these systems of faint concentric rings is displayed by NGC 6543 (Balick, Wilson, & Hajian 2000). In reality, they are regularly spaced concentric shells, indicating quasi-periodic events with time intervals, assuming typical expansion velocities of AGB winds, in the range of 500 to 1500 years. These time scales are too short for thermal pulses and too long for acoustic envelope pulsations and, thus, the origin of the rings cannot be ascribed to any of this type of events. Soker (2000) made a critical review of the mechanisms that have been proposed to explain them, and he indicates that mass-loss variations associated with solar-like magnetic cycles are perhaps the best alternative for their origin.

García-Segura et al. (2001) presented 2(1/2)D magnetohydrodynamic numerical simulations of the

effects of a solar-like magnetic cycle, with periodic polarity inversions, in the slow wind of an AGB star. The stellar wind is modeled with a steady mass-loss at constant velocity. This simple version of a solar-like cycle, without mass-loss variations, is able to reproduce many properties of the observed concentric rings. The shells are formed by pressure oscillations, which drive compressions in the magnetized wind. These pressure oscillations are due to periodic variations in the field intensity. The periodicity of the shells, then, is simply a half of the magnetic cycle since each shell is formed when the magnetic pressure goes to zero during the polarity inversion. As a consequence of the steady mass-loss rate, the density of the shells scales as r^{-2} , and their surface brightness has a steeper drop-off, as observed in the shells of NGC 6543, the best documented case of these HST rings. Deviations from sphericity can be generated by changing the strength of the magnetic field. For sufficiently strong fields, a series of symmetric and equidistant blobs are formed at the polar axis, resembling the ones observed in He 2-90. These blobs are originated by magnetic collimation within the expanding AGB wind.

G.G.-S. thanks Michael L. Norman and the Laboratory for Computational Astrophysics for the use of ZEUS-3D. All computations were performed at Instituto de Astronomía-Universidad Nacional Autónoma de México. This work has been partially supported by grants from DGAPA-UNAM (IN130698, IN117799 & IN114199) and CONACyT (32214-E).

REFERENCES

- Acker, A., Fresneau, A., Pottasch, S. R., & Jasiewicz, G. 1998, *A&A*, 337, 253
- Balick, B., Wilson, J., & Hajian, A. R. 2000, *AJ*, 121, 354
- Bochkarev, N. G. 1988, *Nature*, 332, 518
- Borison, B., McCray, R., Clark, C. O., Slavin, J., Mac Low, M., Chu, Y., & Van Buren, D. 1997, *ApJ*, 478, 638
- Chevalier, R. A., & Luo, D. 1994, *ApJ*, 421, 225
- Chita, S. M., van Marle, A. J., Langer, N., & García-Segura, G. 2007, *RevMexAA (SC)*, 30, 80
- Chu, Y.-H., Guerrero, M. A., Gruendl, R. A., García-Segura, G., & Wendker, H. J. 2003, *ApJ*, 599, 1189
- Clarke, D. A. 1996, *ApJ*, 457, 291
- García-Díaz, M. T., López, J. A., García-Segura, G., Richer, M. G., & Steffen, W. 2008, *ApJ*, 676, 402
- García-Segura, G. 1997, *ApJ*, 489, L189
- García-Segura, G., & Mac Low, M.-M. 1995, *ApJ*, 455, 145
- García-Segura, G., Langer, N., & Mac Low, M.-M. 1996a, *A&A*, 316, 133
- García-Segura, G., Mac Low, M.-M., & Langer, N. 1996b, *A&A*, 305, 229
- García-Segura, G., Langer, N., Różyczka, M., & Franco, J. 1999a, *ApJ*, 517, 767
- García-Segura, G., Langer, N., Różyczka, M., Franco, J., & Mac Low, M.-M. 1999b, *IAU Symp.* 193, *Wolf-Rayet Phenomena in Massive Stars and Starburst Galaxies*, ed. K. A. van der Hucht, G. Koenigsberger, & P. R. J. Eenens (San Francisco: ASP), 325
- García-Segura, G., López, J. A., & Franco, J. 2001, *ApJ*, 560, (28)
- García-Segura, G., López, J. A., & Franco, J. 2005, *ApJ*, 618, 919
- García-Segura, G., López, J. A., Steffen, W., Meaburn, J., & Manchado, A. 2006, *ApJ*, 646, L61
- Goldman, D. B., Guerrero, M. A., Chu, Y.-H., & Gruendl, R. A. 2004, *AJ*, 128, 1711
- Hrivnak, B. J., Kwok, S., & Su, K. Y. L. 2001, *AJ*, 121, 2775
- Jordan, S., Werner, K., & O'Toole, S. J. 2005, *A&A*, 432, 273
- Kaler, J. B., Shaw, R. A., & Kwitter, K. B. 1990, *ApJ*, 359, 392
- Kwok, S., Su, K. Y. L., & Hrivnak, B. J. 1998, *ApJ*, 501, L117
- Méndez, R. H., & Niemela, V. S. 1977, *MNRAS*, 178, 409
- Pérez-Rendón, B., García-Segura, G., & Langer, N. 2009, *A&A*, in press (arXiv:0905.1101)
- Różyczka, M., & Franco, J. 1996, *ApJ*, 469, L127
- Soker, N. 2000, *ApJ*, 540, 436
- Stone, J. M., & Norman, M. L. 1992, *ApJS*, 80, 753
- Terzian, Y., & Hajian, A. R. 2000, in *ASP Conf. Ser.* 199, *Asymmetrical Planetary Nebulae II: From Origins to Microstructures*, ed. J. H. Kastner, N. Soker, & S. A. Rappaport (San Francisco: ASP), 33
- Traulsen, I., Hoffmann, A. I. D., Rauch, T., Werner, K., Dreizler, S., & Kruk, J. W. 2005, *ASP Conf. Ser.* 334, *14th European Workshop on White Dwarfs*, ed. D. Koester & S. Moehler (San Francisco: ASP), 325
- van Marle, A. J., et al. 2008, *A&A*, 478, 769
- van Marle, A. J., Langer, N., Achterberg, A., & García-Segura, G. 2006, *A&A*, 460, 105
- van Marle, A. J., Langer, N., & García-Segura, G. 2005, *A&A*, 444, 837
- Villaver, E., García-Segura, G., & Manchado, A. 2002a, *ApJ*, 571, 880
- Villaver, E., Manchado, A., & García-Segura, G. 2002b, *ApJ*, 581, 1204
- Weaver, R., McCray, R., Castor, J., Shapiro, P., & Moore, 1977, *ApJ* 218, 377
- Wehmeyer, R., & Kohoutek, L. 1979, *A&A*, 78, 39